Absorbed Power Distributions from Coherent Microwave Arrays for Localized Hyperthermia

J. W. HAND, J. L. CHEETHAM, AND A. J. HIND

Abstract—**Absorbed power distributions in a homogeneous muscle-like tissue due to a planar coherent array consisting of 16 small direct contact applicators at 434 and 915 MHz are calculated, assuming various relative phases and amplitudes are compared with that of a single aperture source at the same frequency with the same overall dimensions. The array applicator may offer improvement in field size or, when focused, a small improvement in penetration, but in practice the performance is very dependent upon bolus thickness. An additional advantage of the array applicator is the ability to modify absorbed power distributions during use by changing the amplitudes of individual applicators.**

I. Introduction

THE USE OF MICROWAVES and radio frequencies in localized hyperthermal treatments of patients with superficial tumors is being investigated in many institutions worldwide and several types of electromagnetic applicators have been described. These include dielectrically-loaded waveguides with rectangular, circular or ridged cross sections [1]–[3], inductive applicators [4], [5], and microstrip-based applicators [6], [7]. Most applicators operate at a frequency within the 100–1000-MHz band and, for dimensions compatible with localized treatment, the penetration depth[1] in muscle-like tissue is usually less than 4 cm. Experience has also shown that distributions of Specific Absorption Rate[2] (SAR) associated with many applicators are such that the effective treatment fields (e.g., defined by the −3-dB contour) can be significantly smaller than the areas defined by the dimensions of the applicators. A further limitation of a single applicator is that the SAR distribution cannot be modified during use, making it difficult to improve the nonuniform temperature distributions that are invariably produced during the treatment of patients.

Manuscript received October 3, 1985; revised January 16, 1986

J. W. Hand and J. L. Cheetham are with the MRC Cyclotron Unit, Hammersmith Hospital, London W12 OHS, England

A. J. Hind is with Siemens Ltd., Sunbury-on-Thames, England.

IEEE Log Number 8607848.

[1] Penetration depth D, is the distance into the tissue at which the electric field is reduced by a factor e. SAR is reduced to 13.5 percent over this distance. The −3-dB power depth d, is also frequently used to describe the performance of hyperthermia applicators ($d = 0.346D$).

[2] SAR is the time derivative of the incremental energy (dw) absorbed by an incremental mass (dm) contained in a volume element (dv) of a given density (ρ) [8].

$$\mathrm{SAR} = \frac{d}{dt}\left[\frac{dw}{dm}\right] = \frac{d}{dt}\left[\frac{dw}{\rho\, dv}\right] \mathrm{W \cdot kg^{-1}}.$$

Because of these shortcomings of current applicators, the potential of a new generation of multielement applicators is being investigated. For example, a cylindrical array of 2450-MHz dipoles placed around the patient [9], a hexagonal planar array of 2450-MHz elements [10], multielement direct contact applicators with curved apertures [11], [12], and a plane rectangular aperture source with a continuous distribution of phase and/or amplitude [13], [14] are among systems that have been considered.

In this paper, SAR distributions in homogeneous muscle-like tissue due to a planar array of small, direct contact applicators are considered. The performance of the array, assuming various relative phases and amplitudes for the elements, is assessed in relation to the SAR distribution of a single aperture source of the same overall dimensions.

II. Method

The array applicator, shown in Fig. 1, is modeled as a 4×4 array of coplanar aperture sources with the electric field on each aperture polarized in the y-direction and varying as $E_c \sin(\pi x/a)$, where a is the dimension of the small aperture in the x direction and E_c is the electric field at $x = a/2$. For a given value of x, the electric field on an aperture is assumed to be independent of y except at the edges where it is zero. The apertures have dimensions 4.0 cm × 4.0 cm and are separated from each other by 1.0 cm. In practice, such small applicators would be loaded with a material having high permittivity. This would not only permit propagation in the applicators at the frequencies considered here (915 and 434 MHz) but would also aid impedance matching to the tissue. The complete array is assumed to be in contact with the plane surface of a semi-infinite region of homogeneous muscle-like tissue. The relative permittivity ϵ of this medium is taken to be $(51 - j25)$ at 915 MHz and $(53 - j49)$ at 434 MHz. The fields at the surface of the tissue are assumed to be zero except beneath the 16 apertures where they are assumed to be equal to those on the apertures. Coupling from the irradiated tissue back to the applicator is neglected as is mutual coupling between applicators.

The electric and magnetic fields on the aperture plane are replaced by $\boldsymbol{J}_{\mathrm{sm}}$, the equivalent magnetic current surface density

$$\boldsymbol{J}_{\mathrm{sm}}(R) = -\boldsymbol{k} \times \boldsymbol{E}(R) \tag{1}$$

0018-9480/86/0500-0484$01.00 ©1986 IEEE

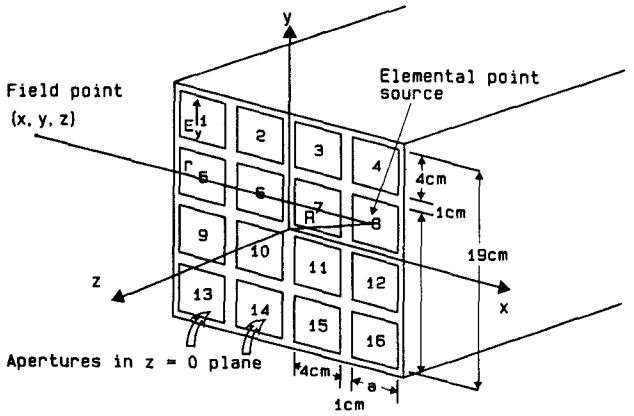

Fig. 1. The array applicator model.

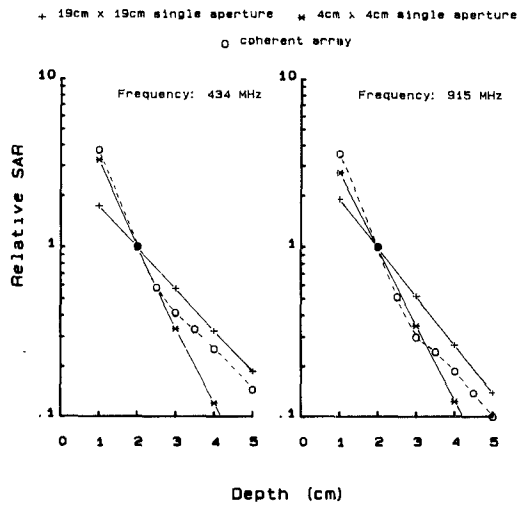

Fig. 2. z-dependence of the peak SAR due to coherent arrays with individual applicators driven in phase with equal amplitudes, a single aperture source with the same dimensions as the array, and an individual applicator from the array.

and J_{se}, the equivalent electric surface current density

$$J_{se}(R) = -k \times H(R). \tag{2}$$

The distribution on the aperture plane is modeled by an array of point source dipoles with appropriate amplitudes and phases [15]. The separation between dipoles in both the x- and y-directions is 5 mm. For each dipole, the magnetic and electric vector potentials A and F are

$$A(R, r) = \frac{\mu_0 \cdot J_{se}(R) e^{-\gamma r}}{4\pi r} \tag{3}$$

and

$$F(R, r) = \frac{\epsilon J_{sm}(R) e^{-\gamma r}}{4\pi r} \tag{4}$$

with $\gamma^2 = -\omega^2 \mu_0 \epsilon$. The fields at any point (x, y, z) $(z > 0)$ due to this point source are

$$E(R, r) = -j\omega A - \frac{j}{\omega \mu_0 \epsilon} \nabla(\nabla \cdot A) - \frac{1}{\epsilon} \nabla \times F \tag{5}$$

$$H(R, r) = -j\omega F - \frac{j}{\omega \mu_0 \epsilon} \nabla(\nabla \cdot F) - \frac{1}{\mu_0} \nabla \times A. \tag{6}$$

The total electric field E_{tot} at (x, y, z) is found by vector addition of the contributions from each elemental point source in the aperture plane. The specific absorption rate at (x, y, z) is proportional to $\hat{E}_{tot}^2$ where $\hat{E}_{tot}$ is the peak value of E_{tot} (x, y, z).

SAR distributions are calculated for coherent arrays operating at 915 and 434 MHz. For comparison, SAR distributions are also calculated at the same frequencies for a 19 cm × 19 cm aperture assuming an electric field polarized in the y-direction and varying as $E_c' \sin(\pi x/19)$, where E_c' is the electric field at $x = 9.5$ cm. Within the aperture, the electric field is independent of y but is zero on all edges.

III. Results

A. Coherent Arrays with Equal Phases and Amplitudes

The SAR distribution, due to the coherent array of small applicators driven in phase with equal amplitudes, peaks sharply beneath each applicator and maximum values decrease rapidly with increasing distance into the tissue. Fig. 2 compares the penetration of the coherent arrays with those of a single applicator of the same dimensions as the array and an individual 4 cm×4 cm element. The peak value of SAR, calculated at a given depth z, is normalized to the maximum in the plane 2 cm deep. In practice, the most superficial tissue could be spared by cooling the skin; normalization at 2 cm was chosen as a compromise between the need to avoid the near-field effects at small z and yet obtain a realistic assessment of the usefulness of the array bearing in mind the reduced effectiveness of skin cooling at greater depths [16]. The small penetration depths associated with electrically small aperture sources and the plane-wave penetration depths of the relatively large apertures have been discussed previously [7], [14], [15]. Fig. 2 shows that the near-field effects for the coherent array are even more dominant than for an individual element, but for $z > 3$ cm, the penetration depth becomes similar to that of a large single applicator, implying that the coherent array would match the penetration achievable with current applicators if a bolus of similar permittivity to the tissue and at least 3 cm thick was inserted between the elements and the tissue. Since the near-field pattern of the array consists of regions of high and low SAR, the simple temperature controlled bolus commonly used in current clinical practice may prove inadequate. Nonuniformly cooled boli have been used occasionally with conventional waveguide applicators, and this concept could be extended to a segmented bolus in which the temperatures of the boli beneath each small applicator could be individually controlled. Since this will require a control system of greater complexity, the cost-effectiveness of such a bolus remains to be evaluated.

Fig. 3(a) shows SAR (x, y) at depth $z = 2$ cm due to the coherent 434-MHz array. The local maximum in SAR produced beneath a centrally located aperture (#6, 7, 10, or 11—see Fig. 1) surrounded by 8 neighboring apertures differs by less than 10 percent from that beneath a corner

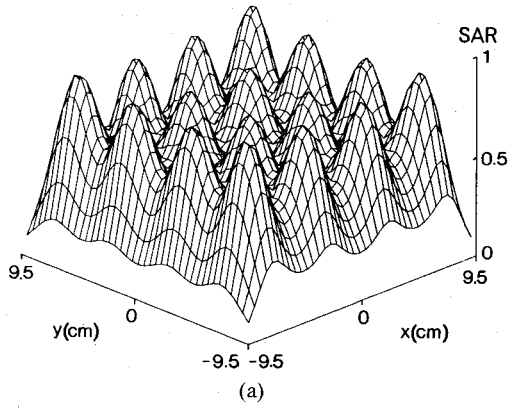

(a)

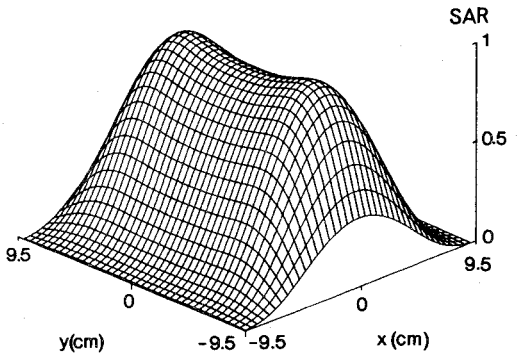

(b)

Fig. 3. (a) SAR (x, y) at depth 2 cm due to 434-MHz array with individual applicators driven in phase with equal amplitudes. (b) SAR (x, y) at depth 2 cm due to the 434-MHz 19 cm×19 cm applicator.

aperture (#1, 4, 13, or 16) with only three neighbors. At this depth, the effect of phase coherence is small and a noncoherent array will produce a similar SAR distribution. However, the effective penetration of a noncoherent array is less than that of a coherent one at depths of 3 cm or more, as the characteristic of an individual 4 cm×4 cm aperture shown in Fig. 2 infers. Fig. 3(b) shows SAR(x, y) at depth $z = 2$ cm due to the 434-MHz single 19 cm× 19 cm aperture. If an array gain factor G defined as

$$G(x, y, z) = \frac{\mathrm{SAR}(x, y, z)_{\text{array}}}{\mathrm{SAR}(x, y, z)_{\text{single applicator}}} \qquad (7)$$

is introduced, the coherent array can be seen to have a marked advantage over the single applicator in that significant levels of absorbed power are produced over a larger area beneath the applicator particularly near the edges as $|x| \to 9.5$ cm. For example, Fig. 4 shows $G(x, y)$ for $z =$ 2 cm, assuming that the maximum values of SAR in this plane for the single large applicator and the coherent array are equal. Fig. 5 shows that the −3-dB contour of the distribution for the coherent array encompasses more than 80 percent of the 19 cm×19 cm area beneath the applicator, compared with approximately 42 percent in the case of the large single aperture. Similar calculations for the 915-MHz coherent array show that its SAR distribution at $z = 2$ cm has more localized peaks and a −3-dB contour which is not contiguous, as illustrated in Fig. 6.

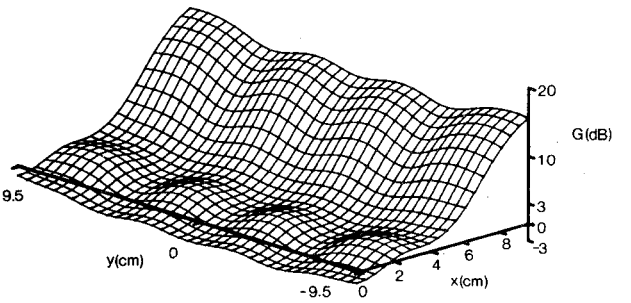

Fig. 4. Array gain factor $G(x, y)$ in plane $z = 2$ cm for the 434-MHz array with individual applicators driven in the phase with equal amplitudes. Values for half the area beneath the applicator ($0 \leqslant x \leqslant 9.5$ cm; $-9.5 \leqslant y \leqslant 9.5$ cm) are shown.

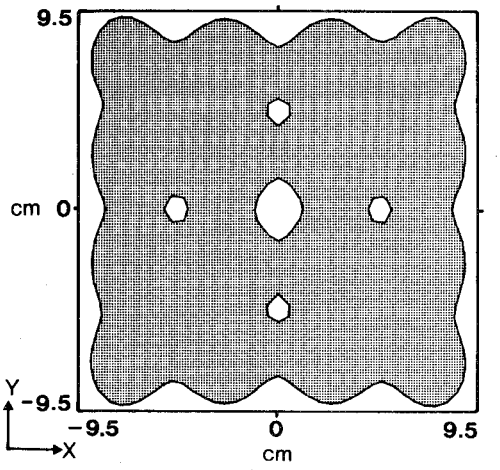

(a)

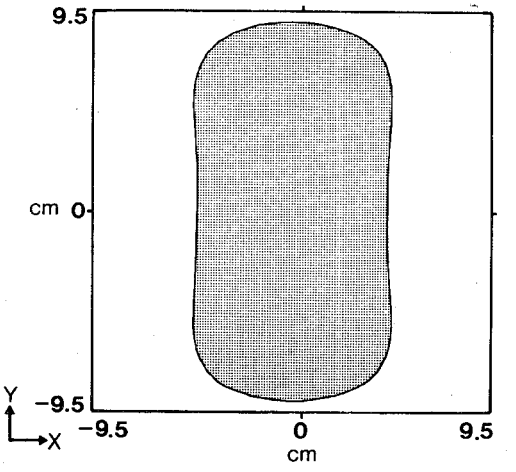

(b)

Fig. 5. −3-dB contours for the SAR distributions shown in Figs. 3(a) and (b). The SAR within the shaded areas ⩾ 50 percent of maximum SAR at $z = 2$ cm. (a) Coherent array. (b) Single applicator.

B. Focused Arrays

To produce a focused field at a point F in the lossy medium, the field contributions from each source must have the same phase at F. For the array considered here, the following condition is set

$$\frac{2\pi r_p'}{\lambda} + \psi_p = \text{constant} \qquad (p = 1, 2, \cdots 16) \qquad (8)$$

where r_p' is the distance between the center of the pth

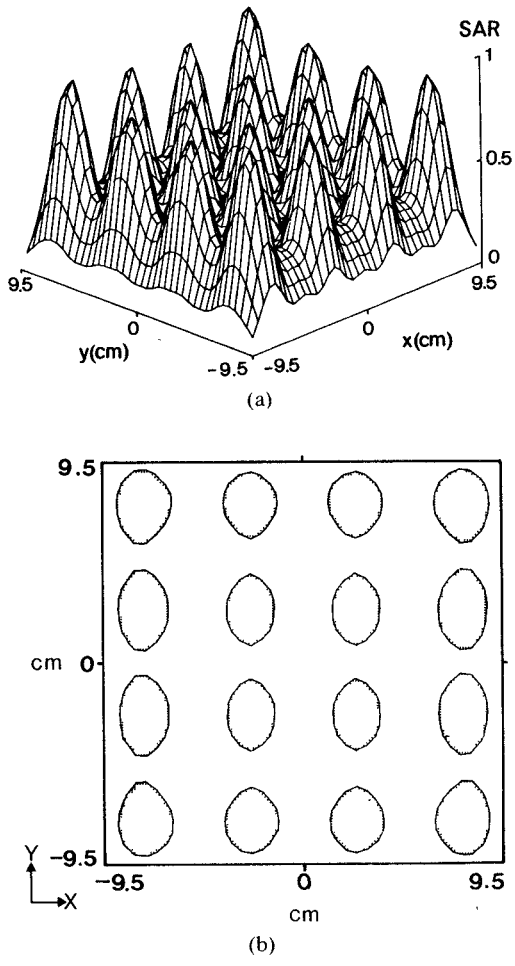

Fig. 6. (a) SAR (x, y) at depth 2 cm due to 915-MHz array with individual applicators driven in phase with equal amplitudes. (b) -3-dB contours showing shaded regions in which SAR ≥ 50 percent maximum SAR at $z = 2$ cm.

aperture and the focus F, λ is the wavelength in the lossy medium, and ψ_p is a phase adjustment for the pth aperture. In the examples discussed below, the focus is on the z-axis and phase adjustments are relative to the four apertures in the center of the array.

The SAR distribution due to the focused array peaks sharply beneath each applicator and the rapid decrease in peak values with increasing distance into the tissue implies that the performance of the array is dependent upon bolus thickness. In Fig. 7, the peak SAR's calculated in the focal planes, normalized to the respective peak SAR at depth 2 cm, are shown for 434- and 915-MHz arrays for foci between 3 and 6 cm. In all cases, the elements of the arrays were assumed to be driven with equal amplitudes. The 434-MHz array achieves a small improvement in penetration compared with the large single aperture when focused at depths greater than about 4 cm. At 915 MHz, however, the relatively local and intense hot spots at depth 2 cm (the plane of normalization assumed for Fig. 7) in the near-field pattern of the array, result in a poorer penetration for the focused array compared with the large single aperture. If normalization is made at a larger value of z (implying the use of a thicker bolus with similar permittivity to that of the tissue), then the 915-MHz array also achieves a small

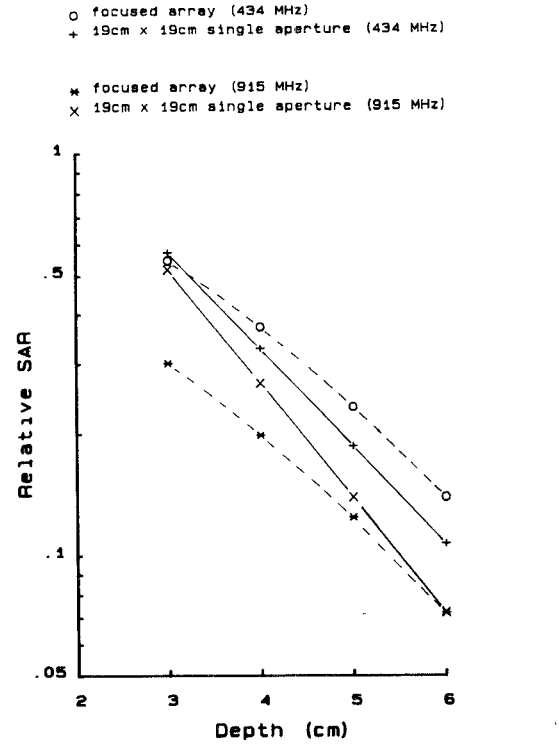

Fig. 7 Peak SAR in focal planes, normalized to peak SAR at $z = 2$ cm, produced by focused arrays. The individual applicators are driven with equal amplitudes. Normalized peak SAR's due to single aperture sources of the same dimensions, calculated at those depths, are also shown.

improvement in penetration compared with the corresponding larger single aperture. For example, we have calculated (but not shown in Fig. 7) that when the peak SAR at depth $z = 4$ cm is taken as a reference value, the gain of the 915-MHz array focused at 6 cm is 1.5 dB with respect to the single aperture.

Fig. 8(a) shows the SAR distribution in the focal plane ($z = 4$ cm), normalized to the peak SAR at depth $z = 2$ cm, for a 915-MHz array in which individual applicators are driven with equal amplitudes. The maximum SAR for $z = 4$ cm is produced at the focus (0,0,4) and the half power widths in the x- and y-directions are, respectively, 0.68 and 0.8 times λ, the wavelength in the tissue. A disadvantage of this illumination is that significant secondary peaks of up to 85 percent of the SAR at the focal point are produced. However, the illumination of the array can be chosen to improve the SAR distribution at the focus if elements distant from it are only weakly excited [14]. Fig. 8(b) and (c) show SAR in the focal planes of 915- and 434-MHz arrays focused at (0,0,4) in which the amplitudes of the electric fields (E_{cp}) at the centers of each applicator are adjusted such that

$$E_{cp}/\exp(-r'_p/D) = \text{constant} \qquad (p = 1,2\cdots 16) \quad (9)$$

where r'_p is the distance from the center of the pth aperture to the focus and D is the plane-wave penetration depth in the tissue is 3.0 cm at 915 MHz and 3.6 cm at 434 MHz.

Thus, relative to the electric field (E_{cc}) at the centers of the four centrally located apertures ($p = 6,7,10,11$—see

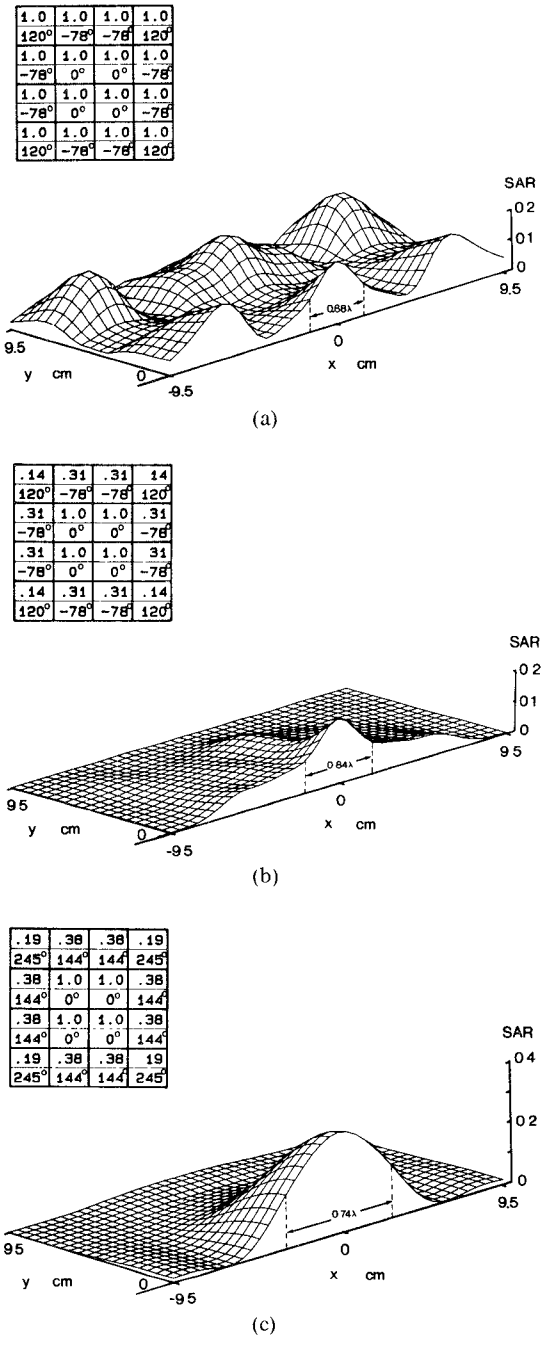

Fig. 8. Relative SAR distributions in the focal plane ($z = 4$ cm) of arrays focused at (0,0,4). In each case, SAR is normalized to the peak value calculated at 2 cm depth. Only half the area beneath the applicator ($0 \leqslant y \leqslant 9.5$ cm; $-9.5 \leqslant x \leqslant 9.5$ cm) is shown. Relative amplitudes (upper figure) and phases in degrees (lower figure) for each applicator are shown in the inserts. (a) 915-MHz array driven with equal amplitudes. (b) 915-MHz array driven with adjusted amplitudes. (c) 434-MHz array driven with adjusted amplitudes.

Fig. 1), E_{cp} is given by

$$E_{cp} = E_{cc} \exp\left(\frac{r_c' - r_p'}{D}\right) \qquad (p = 1,2 \cdots 16) \qquad (10)$$

where r_c' is the distance from the center of the centrally located aperture to the focus. The distribution in Fig. 8(b) shows a small increase (~ 5 percent) in the maximum value, increased half power widths (0.84λ in x; 1.1λ in y) and reduced sidelobes (-5.5 dB with respect to the SAR at the focus) when compared with the case in which the applicators are all driven with equal amplitudes. At 434 MHz (Fig. 8(c)), the half power width of the focus is 0.74λ (in x and y) and sidelobes are -12 dB with respect to the SAR at the focus.

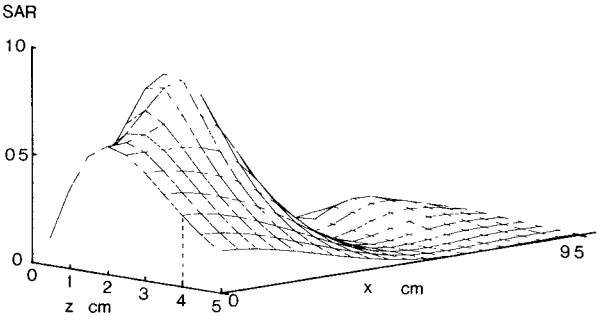

Fig. 9. SAR (x, y), normalized to the peak value in the plane 2 cm deep, due to 434-MHz amplitude adjusted array focused at (0,0,4) for $0 \leqslant x \leqslant 9.5$ cm; $y = 0$; $0.5 \leqslant z \leqslant 5$ cm.

Although the maximum SAR in the focal plane is produced at the focus, the SAR associated with the focused array decreases with increasing depth into the tissue for other values of z in the region of the focal plane. As an example, the z dependence of SAR for the amplituded adjusted 434-MHz array focused at $z = 4$ is shown in Fig. 9. A characteristic of this distribution is the local maximum in the SAR profile along the z axis, the position of which is dependent upon the depth of the focal plane, but is usually located 1.5–2.5 cm from the surface. A similar profile has been described for another focused system [13], but the local nature of the maximum, as indicated in this study and others [14], [17], should be stressed.

IV. Discussion

The results indicate that a coherent unfocused array of direct contact applicators may produce a SAR distribution which gives a larger field size than a single aperture applicator with the same overall dimensions, and that a focused array can produce a two-dimensional focus with a half power width in the focal plane of approximately 0.7–0.8 λ. The performance of the array is dependent upon the near-field effects up to 4 cm from the aperture plane and in practice, a high permittivity bolus would need to be an integral part of the array applicator. Of the two frequencies considered, 434 MHz appears to be a better choice in that greater penetration and, due to the longer wavelength, a more uniform SAR distribution may be achieved. In practice, operating at the lower frequency would decrease reflections from fat layers [7] as well as the sensitivity of the phase conditions for focusing on tissue inhomogeneities. A preliminary study [18] suggested that no advantage is to be gained in operating the array applicator at 300 MHz. The present calculations indicate that, in the presence of bolus, focused arrays should achieve a small gain compared with single aperture applicators with the same dimensions. The predictions are comparable with those in [12], but are more pessimistic than those reported previously for a 20 cm × 20 cm planar applicator focused by a continuous distribu-

tion of phase and spaced from the tissue by 4 cm of low loss bolus [13].

The geometry of the array considered here is chosen for compatibility with typical dimensions of microwave applicators currently in clinical use. Hexagonal packing [10], [19] and different spacing between individual applicators may lead to improved performance. The restriction that each applicator has the same field polarization also could be removed. The use of nonplanar arrays may prove useful since some improvement in size and uniformity of the treatment field has been demonstrated using two tilted applicators [20].

The increased cost and complexity of providing dynamic focusing appears unwarranted with the arrays discussed here because of the two-dimensional nature of the foci produced. The relative phase adjustments to individual applicators could be achieved through the use of suitable feed cables. At the frequencies considered, a tolerance of $\pm \pi/5$ in relative phases produced insignificant changes in the SAR distribution of homogeneous tissue [18]. A relaxation on differential phase tolerances also has been reported for a 2450-MHz system focusing in layered media [10]. To our knowledge, no estimate of phase tolerance for focusing in heterogeneous tissue is available although the concept of focusing at 915 MHz in such media has been demonstrated [21].

The array applicator can offer improvement in field size or, when focused, a small improvement in penetration over single applicators currently used in clinical hyperthermia, but the performance is very dependent upon bolus thickness. The ability to change the amplitude of individual applicators during use should prove to be a marked practical advantage.

Acknowledgment

We thank J. R. James and R. H. Johnson of the Royal Military College of Science, Shrivenham, UK, for their interest and discussions on this topic. We also express our thanks to the reviewers for their helpful comments and suggestions.

References

[1] A. W. Guy, J. F. Lehmann, J. B. Stonebridge, and C. C. Sorensen, "Development of a 915-MHz direct contact applicator for therapeutic heating of tissues," *IEEE Trans. Microwave Theory Tech.*, vol. MTT-26, pp. 550–556, Aug. 1978.

[2] J. C. Lin, G. Kantor, and A. Ghods, "A class of new microwave therapeutic applicators," *Radio Sci.*, vol. 17, pp. 119s–123s, Sept./Oct. 1982.

[3] P. F. Turner, "Electromagnetic hyperthermia devices and methods," M. S. Thesis, Univ. of Utah, pp. 34–39, June 1983.

[4] J. Bach Andersen, A. Baun, K. Harmark, L. Heinzl, P. Raskmark, and J. Overgaard, "A hyperthermia system using a new type of inductive applicator," *IEEE Trans. Biomed. Eng.*, vol. BME-31, pp. 21–27, Jan. 1984.

[5] H. Kato and T. Ishida, "A new inductive applicator for hyperthermia," *J. Microwave Power*, vol. 18, no. 4, pp. 331–336, 1983.

[6] E. Tanabe, A. McEwen, C. S. Norris, P. Fessenden, and T. U. Samulski, "A multielement microstrip antenna for local hyperthermia," in *IEEE 1983 MTT-S Int. Microwave Symp. Dig.*, pp. 183–185, 1983.

[7] R. H. Johnson, J. R. James, J. W. Hand, J. W. Hopewell, P. R. C. Dunlop, and R. J. Dickinson, "New low-profile applicators for local heating of tissues," *IEEE Trans. Biomed. Eng.*, vol. BME-31, pp. 28–37, Jan. 1984.

[8] *Radiofrequency Electromagnetic Fields: NCRP Rep. no. 67*, National Council on Radiation Protection and Measurements, Washington, DC, p. 15, Mar. 1981.

[9] M. Melek, A. P. Anderson, B. H. Brown, and J. Conway, "Measurements substantiating localized microwave hyperthermia within a thorax phantom," *Electron. Lett.*, vol. 18, pp. 437–438, May 1982.

[10] W. Gee, S. W. Lee, N. K. Bong, C. A. Cain, R. Mittra, and R. L. Magin, "Focused array hyperthermia applicator: Theory and experiment," *IEEE Trans. Biomed. Eng.*, vol. BME-31, pp. 38–46, Jan. 1984.

[11] Y. Nikawa, M. Iwamoto, S. Mori, and M. Kikuchi, "Waveguide applicator with convergent lens for localized microwave hyperthermia," *Electron. Commun. Japan*, vol. 66-B, no. 8, pp. 91–98, 1983.

[12] Y. Takahashi, Y. Nikawa, S. Mori, M. Nakagawa, and M. Kikuchi, "Electromagnetic field convergent applicator for microwave hyperthermia at 433 MHz," in *Hyperthermia in Cancer Therapy*, M. Abe *et al.*, Eds. Tokyo: Mag Bros. Inc., pp. 132–133, 1985.

[13] H. Ling, S. W. Lee, and W. Gee, "Frequency optimization of focused microwave hyperthermia applicators," *Proc. IEEE*, vol. 72, pp. 224–225, Feb. 1984.

[14] J. Bach Andersen, "Theoretical limitations on radiation into muscle tissue," *Int. J. Hyperthermia*, vol. 1, pp. 45–55, Jan./Mar. 1985.

[15] P. F. Turner and L. Kumar, "Computer solution for applicator heating pattern," in *National Cancer Institute Monograph 61*, L. A. Dethlefsen, Ed. Bethesda, MD: NIH Publication 82-2437, pp. 521–523, 1982.

[16] J. W. Hand, J. L. Ledda, and N. T. S. Evans, "Considerations of radiofrequency induction heating for localized hyperthermia," *Phys. Med. Biol.*, vol. 27, pp. 1–16, Jan. 1982.

[17] C. T. Tsai, C. H. Durney, and D. A. Christensen, "Calculated power absorption patterns for hyperthermia applicators consisting of electric dipole arrays," *J. Microwave Power*, vol. 19, pp. 1–13, Jan. 1984.

[18] J. W. Hand, A. J. Hind, and J. L. Cheetham, "Multielement microwave array applicators for localized hyperthermia," *Strahlentherapie*, vol. 161, p. 535, Sept. 1985.

[19] E. C. Burdette, T. Benson, R. L. Magin, J. Loane, and S. W. Lee, "Patch antenna phased-array microwave hyperthermia applicator," presented at 33rd Annual Meeting Radiation Res. Soc., Los Angeles, CA, May 5–9 1985. See also Abstract Book, p. 12, -Ad-16.

[20] P. Nilsson, T. Larsson, and B. Persson, "Absorbed power distributions from two tilted waveguide applicators," *Int. J. Hyperthermia*, vol. 1, pp. 29–43, Jan./Mar. 1985.

[21] G. Arcangeli, P. P. Lombardini, G. A. Lovisolo, G. Marsiglia, and M. Piattelli, "Focusing of 915-MHz electromagnetic power on deep human tissues: A mathematical model study," *IEEE Trans. Biomed. Eng.*, vol. BME-31, pp. 47–52, Jan. 1984.

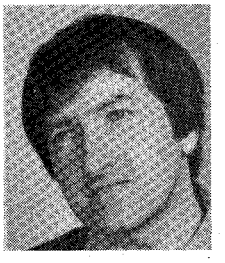

J. W. Hand was born in Derby, England, on June 13, 1946. He received the degree in physics (Hons.) in 1967 and the Ph.D. degree in 1972, both from the University of Newcastle-upon-Tyne, Newcastle-upon-Tyne, England.

In 1976, he joined the staff of the Medical Research Council Cyclotron Unit, Hammersmith Hospital, London, where he is currently an MRC Senior Scientist. His research interests are in the physical aspects of hyperthermia, including electromagnetic heating, ultrasound heating, and thermometry.

J. L. Cheetham, photograph and biography unavailable at the time of publication.

A. J. Hind, photograph and biography unavailable at the time of publication.